Therapeutics

ORIGINAL RESEARCH COMMUNICATION

Inhibition of Carbonyl Reductase 1 Safely Improves the Efficacy of Doxorubicin in Breast Cancer Treatment

Ara Jo,[1],* Tae Gyu Choi,[1],* Yong Hwa Jo,[1],* K.R. Jyothi,[1] Minh Nam Nguyen,[1] Jin-Hwan Kim,[1] Sangbin Lim,[1] Muhammad Shahid,[1] Salima Akter,[1] Seonmin Lee,[1] Kyung Hye Lee,[2] Weon Kim,[2] Hyuck Cho,[3] Juhie Lee,[3] Kevan M. Shokat,[4] Kyung-Sik Yoon,[1] Insug Kang,[1] Joohun Ha,[1] and Sung Soo Kim[1]

Abstract

Aims: Doxorubicin (DOX) is a chemotherapeutic drug that is used to treat many cancers, but its use is limited by cardiotoxic side effect. Carbonyl reductase 1 (CBR1) is an NADPH-dependent oxidoreductase that reduces DOX to doxorubicinol (DOXOL), a less potent derivative that is responsible for DOX cardiotoxicity. Thus, we aimed to demonstrate that inhibition of CBR1 enhances the chemotherapeutic efficacy of DOX and attenuates cardiotoxicity.
Results: Pharmacological or genetic inhibition of CBR1 improved the anticancer effects of DOX in preclinical models of breast cancer. RNA interference or chemical inhibition of CBR1 improved the anticancer effect of DOX in breast cancer. Moreover, CBR1 overexpression enabled breast cancer cells to obtain chemotherapeutic resistance to DOX treatment. Intriguingly, inhibition of CBR1 decreased DOX-induced cardiotoxicity in animal model.
Innovation and Conclusions: Inhibition of CBR1 increases chemotherapeutic efficacy of DOX and reduces cardiotoxicity by blocking DOX reduction to DOXOL. Therefore, we offer preclinical proof-of-concept for a combination strategy to safely leverage the efficacy of doxorubicin by blunting its cardiotoxic effects that limit use of this cytotoxic agent used widely in the oncology clinic. *Antioxid. Redox Signal.* 26, 70–83.

Keywords: carbonyl reductase 1, doxorubicin, doxorubicinol, breast cancer, chemotherapy, cardiotoxicity

Introduction

BREAST CANCER is the leading cause of cancer-related mortality in women, with an estimated 1.7 million cases diagnosed globally, and ~521,900 deaths per year (25% of all cancer cases and 15% of cancer-related deaths) (42). In addition, the overall incidence of breast cancer is increasing, which is likely due to heterogeneity of genetic alterations, several environmental factors, and drug resistance within individual patients (12, 37). Hence, development of novel drug targets is needed for the effective treatment of breast cancer patients.

Doxorubicin (DOX), an anthracycline antibiotic derived from *Streptomyces peucetius var. caesius* (3), is one of the most effective chemotherapeutic agents in the primary treatment of breast cancer (19, 21, 47). DOX intercalates between DNA base pairs, resulting in conformational changes in DNA structure. It prevents DNA and RNA synthesis by inhibiting the activity of topoisomerase II (Topo II) (23). DOX also

generates reactive oxygen species (ROS), such as superoxide ($O_2^{\bullet-}$), hydrogen peroxide (H_2O_2), and hydroxyl radicals ($^\bullet OH$), *via* the interaction with iron during intracellular metabolism, which plays a critical role in cancer cell death (10,

Innovation

Carbonyl reductase1 (CBR1) is an NADPH-dependent oxidoreductase that reduces doxorubicin (DOX) to doxorubicinol (DOXOL), which has less potent anticancer effects than DOX and leads to chronic cardiotoxicity. Inhibition of CBR1 enhances the chemotherapeutic efficacy of DOX and attenuates cardiotoxicity by blocking DOX reduction to DOXOL. This study offers preclinical proof-of-concept for a combination strategy to safely increase the efficacy of doxorubicin by blunting its cardiotoxicity that limits the use of this agent.

[1]Department of Biochemistry and Molecular Biology, School of Medicine, Kyung Hee University, Seoul, Republic of Korea.
[2]Division of Cardiology, Department of Internal Medicine, School of Medicine, Kyung Hee University, Seoul, Republic of Korea.
[3]Department of Pathology, School of Medicine, Kyung Hee University, Seoul, Republic of Korea.
[4]Department of Cellular and Molecular Pharmacology, University of California, San Francisco, California.
*The authors contributed equally to this work.

50). Moreover, DOX is believed to cause dose-dependent inhibition of mitochondrial oxidative phosphorylation (10, 52).

One of the major adverse effects of DOX is cardiotoxicity (29, 46, 51), which limits its use in breast cancer patients. In clinical practice, cumulative doses of DOX can induce irreversible cardiotoxicity, resulting in congestive heart failure (25, 38). Cardiotoxicity is associated with a poor prognosis and high mortality rate. A metabolite of DOX, DOXOL, which is reduced at the side chain C-13 carbonyl moiety of DOX, has been implicated in DOX-induced cardiotoxicity (7, 35). DOXOL has less DNA binding affinity (34) and, thus, exhibits lower chemotherapeutic efficacy than DOX. Several enzymes are involved in the reduction of DOX to DOXOL, including carbonyl reductase 1 (CBR1) (13) and aldo-keto reductase (AKR1C3 and AKR1A1) (13, 32), and may serve as therapeutic targets in ameliorating the cardiotoxicity of DOX.

CBR1 is an NADPH-dependent enzyme of the short-chain dehydrogenases/reductase (SDR) protein family and is widely distributed in human tissues. It can efficiently reduce quinones, prostaglandins, and other carbonyl-containing compounds, including xenobiotics. CBR1 also inactivates lipid aldehydes such as the highly reactive and genotoxic 4-oxonon-2-enal (ONE), 4-hydroxynon-2-enal, and acrolein to less reactive metabolites during oxidative stress (4, 36). Interestingly, CBR1-overexpressing transgenic mice have decreased survival and increased heart damage after DOX treatment (11), which is likely a result of increased DOXOL production. In contrast, conversion from DOX to DOXOL is decreased to an almost undetectable level in CBR1±mice, resulting in reduced cardiotoxicity (34). It has also been reported that the activity of CBR1 is relatively high in human breast and lung cancer patient tissues when compared to normal subjects (24).

In this study, pharmacological inhibition of CBR1 is shown to enhance the chemotherapeutic efficacy of DOX in breast cancers and simultaneously ameliorate cardiotoxicity. Therefore, we propose that CBR1 is a valuable target molecule for future drug development in patients with breast cancer.

Results

Combined treatment with the specific inhibitor of CBR1 (OH-PP-Me) and DOX enhances the chemotherapeutic effect of DOX in breast cancer cells

To determine whether CBR1 inhibition enhanced cell death during DOX treatment, we utilized MDA-MB-157, MDA-MB-436, MCF-7, and MCF10A cell lines, which are triple-negative/basal-B mammary carcinoma, ER-positive/PgR-positive luminal mammary carcinoma, and normal breast cell lines, respectively. MDA-MB-157, MDA-MB-436, and MCF-7 cells have higher CBR1 expression levels than MCF10A (Supplementary Fig. S1A; Supplementary Data are available online at www.liebertpub.com/ars). All of the cell lines were treated with 20 nM DOX. Effects on cell survival were also observed in a combined treatment with 8 μM OH-PP-Me. OH-PP-Me alone did not affect cell viability; however, combination treatment of DOX and OH-PP-Me increased cell death compared to DOX alone in all cell lines (Fig. 1A and Supplementary Fig. S1B). However, there was no significant difference in MCF10A cell viability after treatment of DOX with or without OH-PP-Me. This is probably due to the low level of CBR1 expression in this cell line.

To confirm the synergistic effect of OH-PP-Me and DOX on the cell death, we performed *in vitro* clonogenic assay. The combination treatment markedly decreased colony formations in MDA-MB-157 and MCF-7 cells, compared to doxorubicin treatment alone (Fig. 1B and Supplementary Fig. S1C). The changes in apoptosis-related proteins were also examined. The expression levels of cleaved PARP and caspase-7 and the expression level of Bax were all significantly increased in combination treatment with DOX and OH-PP-Me in cancer cell lines (Fig. 1C and Supplementary Fig. S1D). Since the MCF-7 cell line has a deficiency in caspase-3 (49), activation of caspase-7 was observed in both cell lines.

To verify the effect of combination treatment on cell death, terminal transferase dUTP nick end-labeling (TUNEL) assays were performed. As expected, TUNEL-positive cells were highly increased in combination treatment with DOX and OH-PP-Me compared with DOX alone (Fig. 1D and Supplementary Fig. S1E). It is well known that DOX induces ROS generation (22, 50), and thus, whether combination treatment affected ROS generation was examined. Combined treatment of DOX with OH-PP-Me increased ROS generation compared with DOX treatment alone (Fig. 1E and Supplementary Fig. S2F, G). Collectively, these results demonstrate that CBR1 inhibition during DOX treatment enhances cell death in breast cancer cells.

Knockdown of CBR1 increases cell death after DOX treatment in breast cancer cells

To further elucidate the role of CBR1, cells with a stable knockdown of CBR1 were constructed using two independent small hairpin RNA (shCBR1) clones in both MDA-MB-157 and MCF-7 cells. CBR1 expression was strongly and similarly suppressed in two clones of knocked down cancer cells, that is, CBR1 shRNA #1 and shRNA #2, in both cell lines (Fig. 2A). Knockdown of CBR1 increased cancer cell death by DOX treatment, as shown by cell viability (Fig. 2B). The expression levels of cleaved PARP and caspase-7 and the expression level of Bax were higher in shCBR1 transfectants than in cells transfected with the scrambled controls after DOX treatment (Fig. 2C). The increased cell death was associated with an increase in ROS (Fig. 2D and Supplementary Fig. S2A) in shCBR1 transfectants. Together, these data clearly show that knockdown of CBR1 enhances DOX-induced cell death in breast cancer cells.

Overexpression of CBR1 protects breast cancer cells against apoptosis during DOX treatment

To further support our hypothesis, stable cell lines that overexpressed CBR1 using MDA-MB-157 and MCF-7 cells were made. CBR1 expression was found to be three-fold higher in stably transfected cells than mock transfectants (Fig. 3A). Overexpression of CBR1 decreased DOX-induced cell death (Fig. 3B) compared to mock controls of both cell lines. In the cells stably overexpressing CBR1, expression levels of cleaved PARP and caspase-7, as well as the expression level of Bax, were lower than in the mock controls after DOX treatment (Fig. 3C). In addition, CBR1-overexpressing transfectants exhibited significant reduction of ROS generation (Fig. 3D and Supplementary Fig. S2B). To further confirm the role of CBR1 in DOX-induced cell death, we constructed the two CBR1-GFP plasmids containing a Wobble mutant cDNA encoding
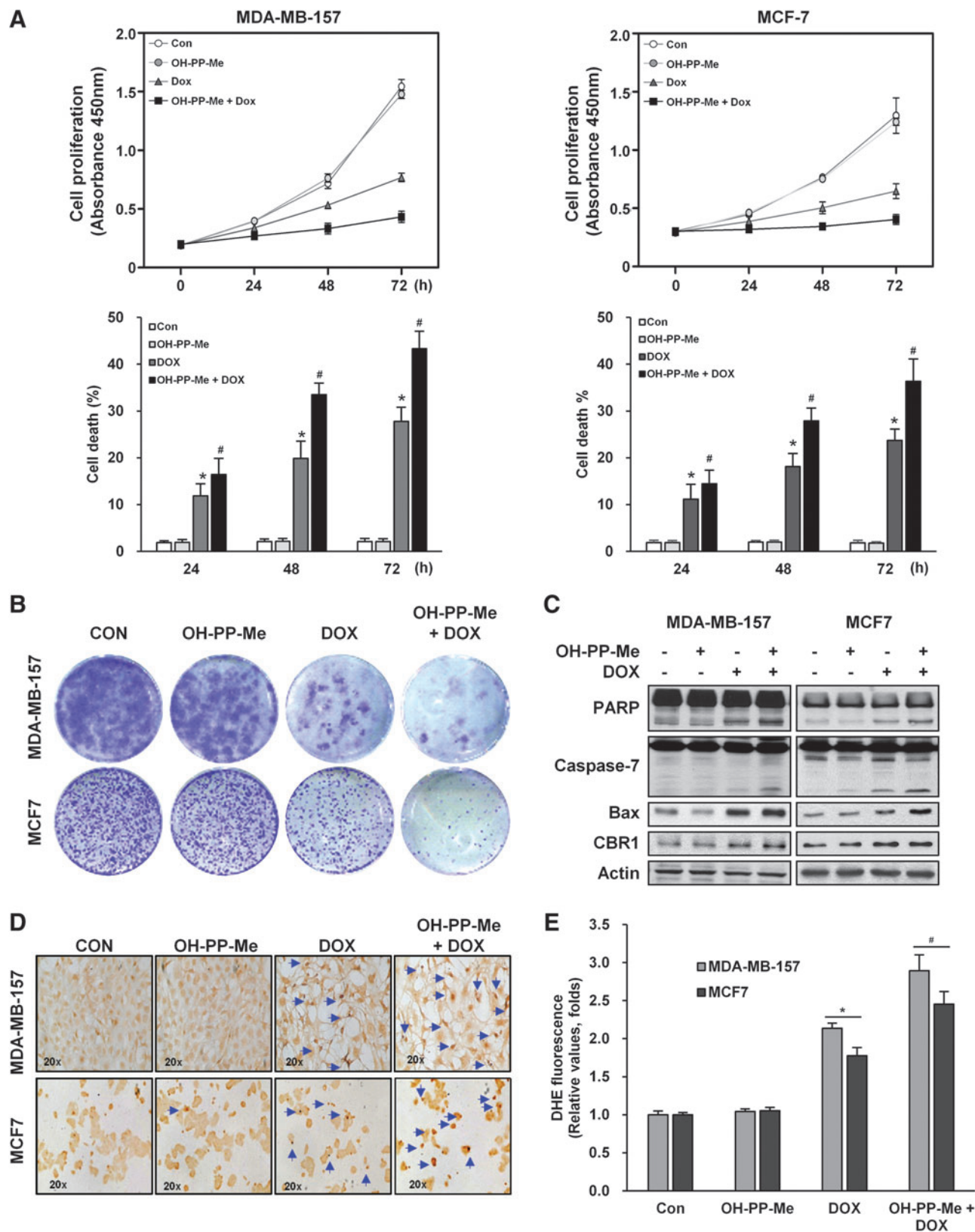
FIG. 1. **The combination of OH-PP-Me and DOX enhances cell death in breast cancer cells.** MDA-MB-157 and MCF-7 cells were treated with 20 nM DOX with or without 8 μM OH-PP-Me for 48 h. **(A)** Cell proliferation and death rates analyzed by the CCK-8 assay and trypan-*blue* exclusion, respectively. *$p < 0.05$ *versus* control cells; #$p < 0.05$ *versus* cells treated with DOX alone. **(B)** Clonogenic assays of MDA-MB-157 and MCF-7 cells. **(C)** Western blot analysis of apoptosis markers. Actin was used as the loading control. **(D)** Apoptosis detected by TUNEL assay. Cells were visualized under confocal microscopy. The *arrows* indicate TUNEL-positive cells. Magnification, 20×. **(E)** ROS measurement. *$p < 0.05$ *versus* control cells; #$p < 0.05$ *versus* cells treated with DOX alone. CON, control; DOX, doxorubicin. Data are representative of at least three different experiments and are expressed as the mean ± SE. CCK-8, cell counting kit-8; ROS, reactive oxygen species; TUNEL, terminal transferase dUTP nick end-labeling; SE, standard error. To see this illustration in color, the reader is referred to the web version of this article at www.liebertpub.com/ars

mouse CBR1 with synonymous point mutations within the shRNA target sequences, and then re-expressed the functional CBR1 in MDA-MB-157 and MCF7 clones harboring the shCBR1 #1 and shCBR1 #2 (Fig. 4A). The re-expression of CBR1 rescued the cells from cell death (Fig. 4B), apoptosis (Fig. 4C), and ROS generation (Fig. 4D and Supplementary Fig. S2C). Overall, these data indicate that overexpression of CBR1 can induce resistance to apoptotic cell death by DOX in breast cancer cells.

CBR1 attenuates DOX-induced oxidative stress in breast cancer cells

To further explore the effect of CBR1 on oxidative stress, cells were pretreated with the ROS scavenger *N*-acetyl-l-cysteine (NAC) for 2 h, and then cell cycle was analyzed for cell death and ROS levels were measured after treatment with DOX and OH-PP-Me. As expected, the combination treatment group with NAC had significantly decreased sub-G1 population and ROS generation compared with the combination treatment group without NAC (Fig. 5A, B). In addition, the results showed a marked reduction in sub-G1population and intracellular ROS levels with NAC and DOX treatment in both scrambled and shCBR1 transfectants (Fig. 5C, D). Consistent results were observed with hydrogen peroxide (H_2O_2) and DOX treatment (Fig. 5E, F). Taken together, these data suggest that CBR1 plays an important role in protecting cells from ROS generation and can cause resistance to DOX treatment in breast cancer cells.

CBR1 inhibitor enhances DOX sensitivity to tumor cells, but prevents cardiotoxicity, in MDA-MB-157 implanted tumor mice

To confirm the effect of combination treatment with OH-PP-Me and DOX on tumor growth *in vivo*, we first established the implanted tumor mouse using the MDA-MB-157 breast cancer cell line. Since tumor masses were observed 2 weeks after the inoculation of MDA-MB-157 cells, mice were injected intraperitoneally with OH-PP-Me (1.67 mg/ kg × 6 times, i.p.), DOX (2.5 mg/kg × 6 times, i.p.), or in combination for 2 weeks. As shown in Figure 6A, the combination treatment of DOX and OH-PP-Me markedly suppressed tumor growth compared with treatment of DOX

alone. In addition, hematoxylin and eosin (H&E) staining of dissected tumor sections revealed that tumor cell number was less in the combination-treated mice group than the DOX-treated group (Fig. 6B). The higher DNA fragmentation was also observed in the tumor specimens from mice cotreated with both compounds compared to those from mice with DOX alone (Fig. 6C).

To determine whether OH-PP-Me could reduce DOX-induced cardiotoxicity in these implanted mice, serum creatine phosphokinase (CPK) levels were measured and cardiac
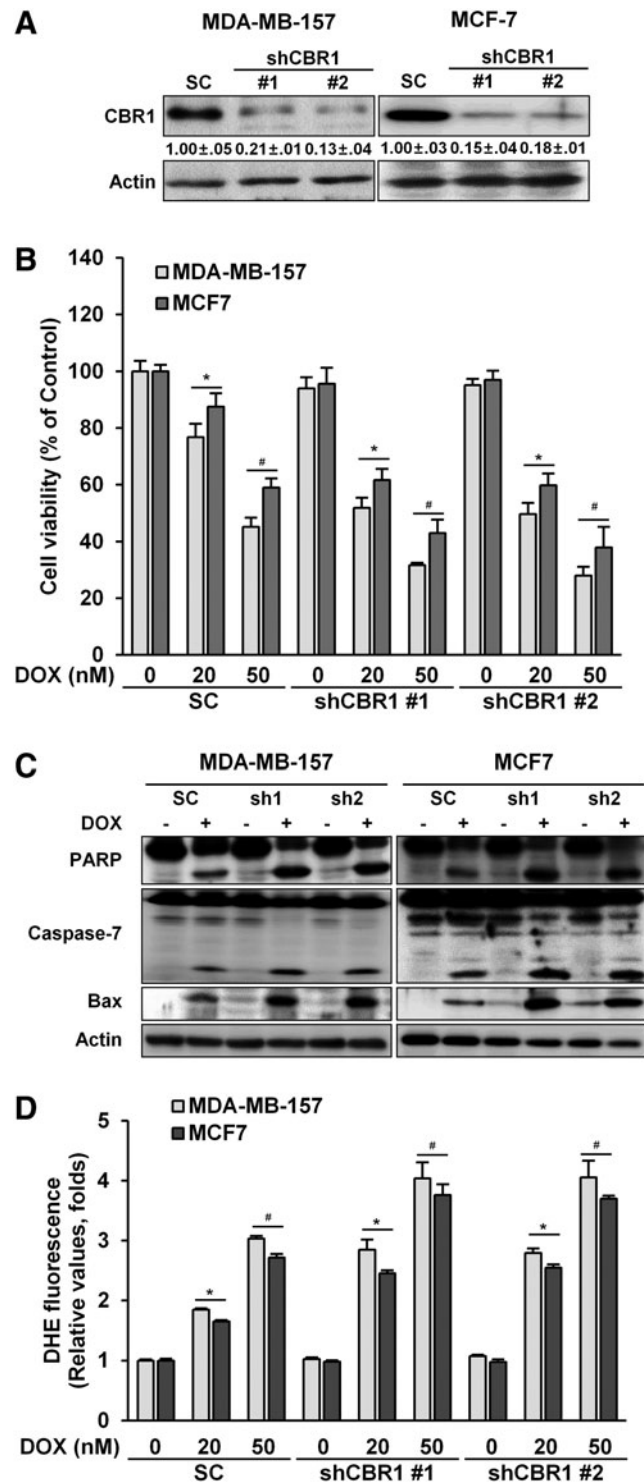
FIG. 2. Knockdown CBR1 increases DOX-induced apoptosis. (A) Western blot analysis. CBR1 protein expression was determined in MDA-MB-157 and MCF-7 cells stably transfected with scrambled or CBR1-specific shRNA. Actin was used as the loading control. **(B)** Cell viability analyzed by CCK-8 assay. Each transfectant was treated with 20 or 50 nM DOX for 48 h. [#]$p < 0.05$ *versus* 20 nM DOX-treated scrambled transfectants; [#]$p < 0.05$ *versus* 50 nM DOX-treated scrambled transfectants. **(C)** Western blot analysis of apoptosis markers. Actin was used as the loading control. **(D)** The ROS level measured by flow cytometry. [#]$p < 0.05$ *versus* 20 nM DOX-treated scrambled transfectants. SC, scrambled; shCBR1, CBR1 shRNA. Data are representative of at least three different experiments and are expressed as mean ± SE. All data are representative of at least three different experiments and are expressed as mean ± SE. CBR1, carbonyl reductase 1; shRNA, small hairpin RNA.

histological tests were performed after dissection. Treatment with DOX alone showed explicit signs of cardiac injuries, whereas the combination of DOX and OH-PP-Me distinctly prevented morphological alterations (Fig. 6D). Moreover, treatment with DOX alone resulted in approximately a three-fold increase in serum CPK activity compared with untreated mice. In contrast, the combination treatment of DOX and OH-PP-Me significantly decreased CPK level in the blood (Fig. 6E). In addition, DOX alone led to a further increase in DNA fragmentation in the cardiac tissues, but the combination of DOX and OH-PP-Me rather reduced DNA fragmentation (Fig. 6F).

Finally, we quantified the apoptosis data to compare cell damage between cardiac and tumor tissues. The quantified results showed that cardiac tissues were more vulnerable to doxorubicin than tumor tissues *as reported previously* (18), and inhibition of CBR1 by OH-PP-ME significantly reduced DNA fragmentation in cardiac tissues while it was enhanced in tumor tissues (Fig. 6G).

We also investigated whether OH-PP-Me could prevent side effects of DOX in heart, blood, and liver using normal mice. Normal mice were treated with the agents in the same manner as the implanted tumor mice, and then H&E staining and complete blood count were performed. In these experiments, DOX induced cardiotoxicity (Supplementary Fig. S3A) and reduced total WBC and platelet numbers (Table 1). To see whether DOX caused the functional and pathological damage in the liver, we performed the blood biochemistry test and H&E staining. The results showed that there was negligible liver damage by DOX *as reported previously* (20). Furthermore, OH-PP-Me alone or combined treatment did not show any functional and pathological damage in the liver (Table 2 and Supplementary Fig. S3B). Overall, these results indicate that inhibition of CBR1 increases the chemotherapeutic effects of DOX and reduces DOX-induced side effect, including heart damage.

OH-PP-Me attenuates DOX-induced cardiotoxicity in a rat model

To further elucidate the effect of OH-PP-Me on DOX-induced cardiotoxicity, a rat model was utilized. Rats are more optimal than mice as an established model for human cardiovascular diseases, as rats have a heart rate that is similar to humans, while mice have a significantly different heart mass, rate, and cell composition of cardiac muscle (1, 5). Cardiac function after DOX (2.5 mg/kg × 6 times, i.p.) treatment with or without the CBR1 inhibitor OH-PP-Me (1.67 mg/kg × 6 times, i.p.) was observed in rats.

FIG. 3. Overexpressed CBR1 decreases DOX-induced apoptosis. (A) Western blot analysis of CBR1 expression. Actin was used as the loading control. **(B)** Cell viability. Each transfectant was treated with 20 or 50 nM DOX for 48 h. [#]$p < 0.05$ *versus* 20 nM DOX-treated mock transfectants; [#]$p < 0.05$ *versus* 50 nM DOX-treated mock transfectants. **(C)** Western blot analysis. Actin was used as the loading control. **(D)** ROS measurement using flow cytometry. [#]$p < 0.05$ *versus* 50 nM DOX-treated mock transfectants. Mock, empty vehicle; CBR1/wt, CBR1 wild type. All data are representative of at least three different experiments and are expressed as mean ± SE.

Serum CPK levels were high after DOX treatment, indicating tissue damage, particularly in cardiac muscle. However, DOX combined with OH-PP-Me significantly decreased the levels of CPK compared with DOX alone (Fig. 7A). Next, H&E staining was used to examine the morphological changes
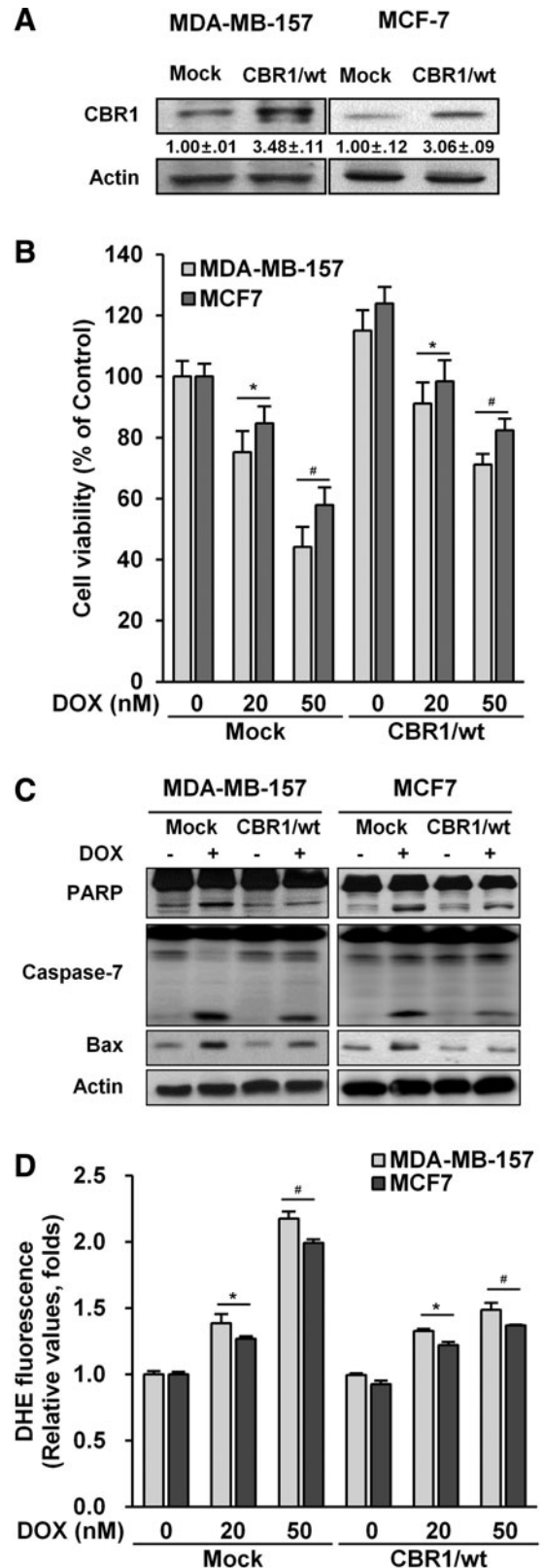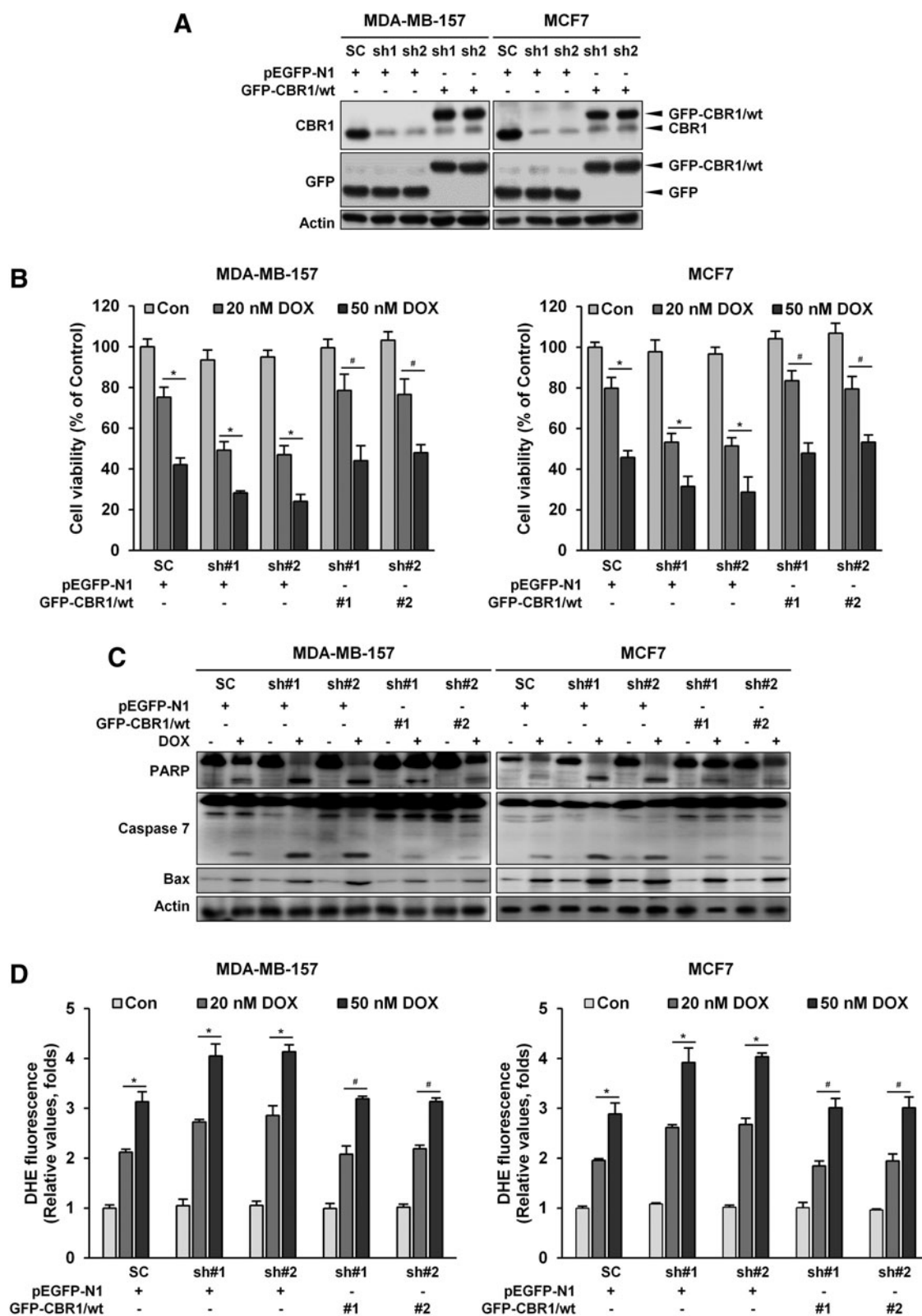
FIG. 4. **Recovered CBR1 decreases cell death, ROS generation, and superoxide level.** **(A)** Western blot analysis. Knockdown CBR1 cell lines were transfected with two distinct CBR1-GFP wild type plasmids. Actin was used as the loading control. **(B)** Cell death analysed by the CCK-8 assay. *$p < 0.05$ *versus* none DOX-treated pEGFP-N1 transfectants; #$p < 0.05$ *versus* DOX-treated pEGFP-N1 transfectants. **(C)** Western blot analysis of apoptosis markers. Actin was used as the loading control. **(D)** The ROS level measured by flow cytometry. All data are representative of at least three different experiments and are expressed as means ± SE. *$p < 0.05$ *versus* none DOX-treated pEGFP-N1 transfectants; #$p < 0.05$ *versus* DOX-treated pEGFP-N1 transfectants.
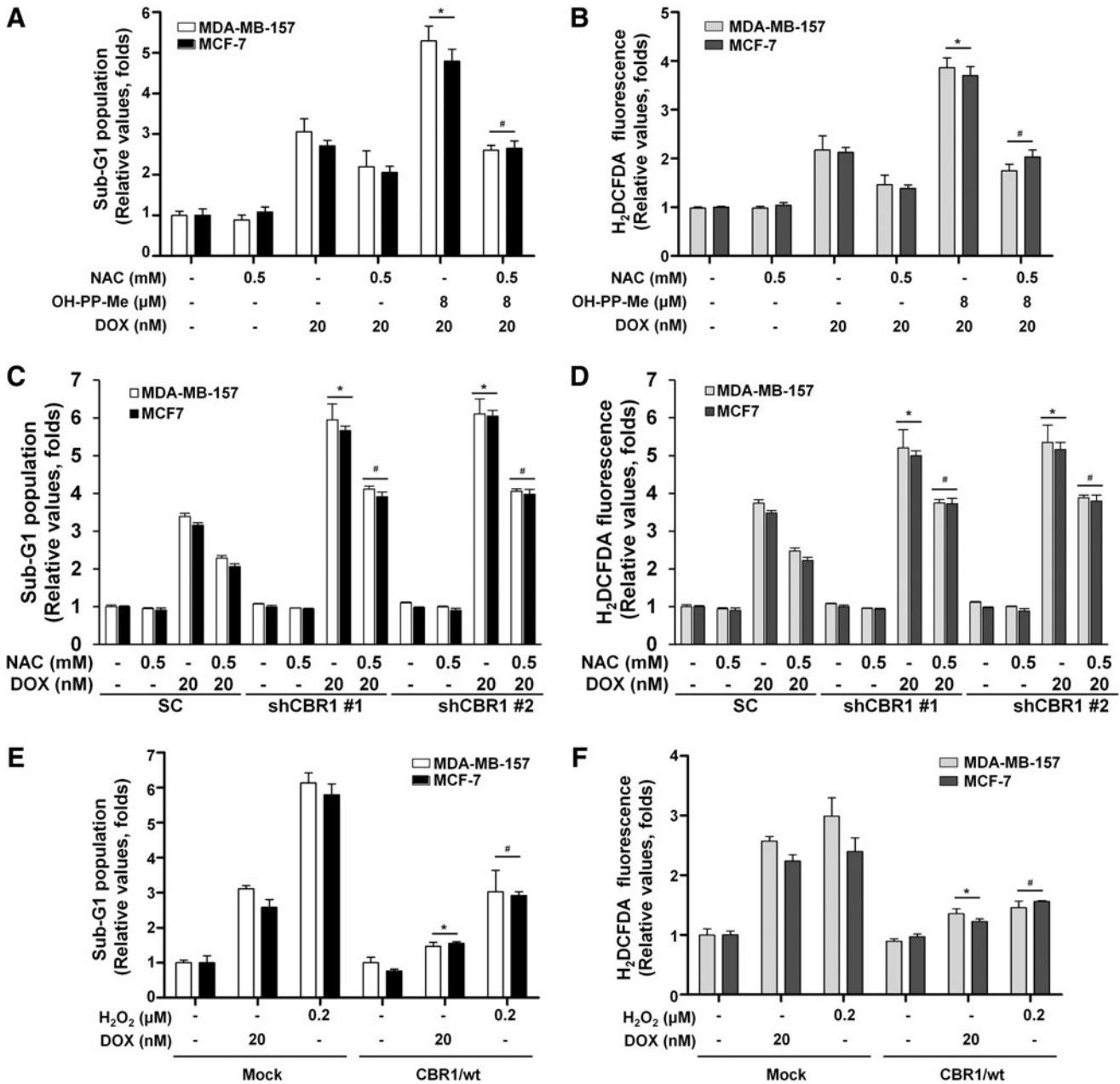
FIG. 5. Effect of CBR1 on DOX-induced ROS generation. (A, B) MDA-MB-157 and MCF-7 cells were pretreated with or without 0.5 mM NAC for 2 h and then treated with 20 nM DOX alone, 8 μM OH-PP-Me alone, or in combination for 48 h. **(A)** Sub-G1 population. **(B)** ROS measurement. *$p < 0.05$ *versus* cells treated with DOX alone; #$p < 0.05$ *versus* cells in combination treatment with 20 nM DOX and 8 μM OH-PP-Me. **(C, D)** Cells stably transfected with scrambled or CBR1-specific shRNA were pretreated with or without 0.5 mM NAC for 2 h, and then treated with or without 20 nM DOX. **(C)** Sub-G1 population. **(D)** ROS measurement. #$p < 0.05$ *versus* DOX-treated CBR1-specific shRNA transfectants. **(E, F)** Cells stably transfected with mock or wild-type CBR1 were treated with either 20 nM DOX or 0.2 mM H_2O_2 for 48 h. **(E)** Sub-G1 population by flow cytometry. **(F)** ROS measurement. #$p < 0.05$ *versus* 20 nM DOX-treated mock transfectants; #$p < 0.05$ *versus* H_2O_2-treated mock transfectants. All data are representative of at least three different experiments and are expressed as the mean ± SE.

associated with drug treatment. Treatment with DOX alone showed overt signs of cardiomyocyte morphological alterations, whereas the combination of DOX and OH-PP-Me markedly rescued morphological alterations (Fig. 7B). In addition, increased DNA fragmentation after exposure to DOX was rescued by OH-PP-Me treatment (Fig. 7C).

Finally, echocardiography results revealed that cardiac function parameters, for example, left ventricular end-

diastolic dimension (LVEDD) and left ventricular end-systolic dimension (LVESD), were increased, but ejection fraction (EF) and fractional shortening (FS) were decreased, during DOX treatment (Fig. 7D). In contrast, the combination treatment showed almost no changes in cardiac function parameters. Collectively, these data demonstrate that cardiomyocyte apoptosis and cardiotoxicity after DOX treatment are decreased when combined with CBR1 inhibitor.
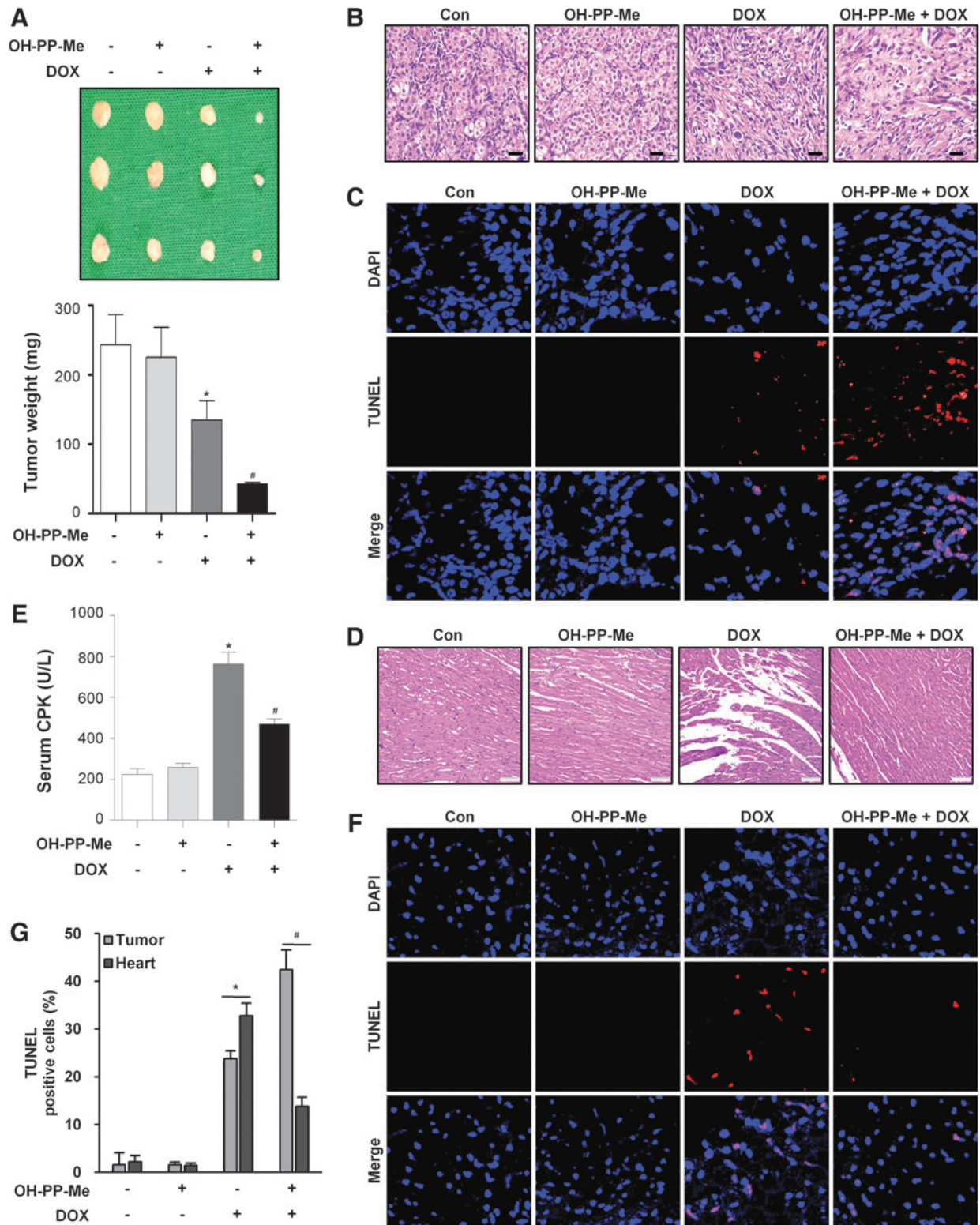
FIG. 6. **CBR1 inhibitor sensitizes tumor cells to DOX and reduces DOX-induced cardiotoxicity in the MDA-MB-157 implantation tumor model.** MDA-MB-157 cells (1×10^7) were injected subcutaneously into the mammary fat pad. The implanted mice were injected intraperitoneally with DOX (2.5 mg/kg) alone, OH-PP-Me (1.67 mg/kg) alone, or in combination every 2 days for 2 weeks. For the combination treatment, mice were injected with OH-PP-Me 1 h post-DOX injection. **(A)** Tumor weight was measured in the indicated groups. *$p < 0.05$ *versus* untreated mice; #$p < 0.05$ *versus* DOX-injected mice. **(B)** H&E staining of implanted tumors. Scale bar, 50 μm. **(C)** TUNEL staining was conducted to detect apoptotic cells in the implanted tumors derived from MDA-MB-157 cells. Nuclei were stained with DAPI. Scale bar, 20 μm. **(D)** H&E staining of heart tissues in mice. Scale bar, 50 μm. **(E)** CPK assay. *$p < 0.05$ *versus* untreated mice; #$p < 0.05$ *versus* DOX-injected mice. **(F)** TUNEL staining. Nuclei were stained with DAPI. Scale bar, 20 μm. **(G)** Histogram of TUNEL-positive cells in the implanted tumor and heart. CPK, serum creatine phosphokinase; H&E, hematoxylin and eosin. To see this illustration in color, the reader is referred to the web version of this article at www.liebertpub.com/ars

TABLE 1. EFFECTS OF DOX AND/OR OH-PP-ME ON COMPLETE BLOOD COUNT

Parameters	Reference range[a]	Control[a]	OH-pp-Me[a]	DOX[a]	OH-pp-Me + DOX[a]
WBC (10^3cells/μl)	1.8–10.7	2.40 ± 0.75	2.00 ± 0.24	**1.53 ± 0.16**	1.86 ± 0.16
RBC (10^6 cells/μl)	6.36–9.42	8.44 ± 0.31	6.17 ± 0.70	8.76 ± 0.61	7.62 ± 0.16
Hemoglobin (g/dl)	11.0–15.1	13.27 ± 0.42	10.43 ± 0.55	14.48 ± 0.80	11.80 ± 0.23
Platelet (10^3/μl)	592–2972	618.33 ± 11.46	704.4 ± 222.47	**405.8 ± 87.31**	737.2 ± 230.10
Neutrophil (%)	6.6–38.9	14.93 ± 2.22	17.82 ± 2.44	14.23 ± 0.84	15.96 ± 2.27
Lymphocyte (%)	55.8–91.6	77.55 ± 2.08	72.00 ± 2.77	77.72 ± 3.36	73.52 ± 4.33
Monocyte (%)	0.0–7.5	2.48 ± 0.20	3.24 ± 0.55	1.72 ± 0.27	2.70 ± 0.75
Eosinophil (%)	0.0–3.9	3.35 ± 0.44	4.22 ± 0.15	**6.98 ± 1.84**	2.65 ± 0.47
Basophil (%)	0.0–2.0	0.22 ± 0.03	0.22 ± 0.04	0.27 ± 0.02	0.18 ± 0.06

[a]Mean ± SE (range).
Bold, out of normal reference range.
DOX, doxorubicin; RBC, red blood cells; WBC, white blood cell; SE, standard error.

Discussion

Breast cancer is one of the most common cancers in women. It is also a major cause of cancer-related death (42), accounting for 15% of all cancer deaths globally in 2012. Breast cancer is a heterogeneous disease influenced by several environmental factors and is susceptible to the development of drug resistance, and thus, the most optimal treatment option still remains undefined (12).

Treatment strategies vary between individuals based on clinical factors such as stage, hormonal status, HER2 overexpression, and comorbidities. Chemotherapy is given as neoadjuvant, adjuvant, or as palliative treatment. The most active agents for breast cancer are anthracyclines and taxanes (27). These drugs are used as single agents or in combination with other agents in various settings. Generally, combination chemotherapy produces better outcomes, although increased toxicities present a major concern (9). Since the targeted agent era, trastuzumab, which targets the HER2 receptor, was introduced for the treatment of HER2-overexpressing breast cancer. Combination of trastuzumab with cytotoxic chemotherapy showed improved outcomes in a prior randomized phase III trial (44).

However, significant cardiotoxicity was a major adverse event. Concomitant use of trastuzumab and DOX is still not recommended because of cardiotoxicity. Furthermore, the combination of DOX with other agents, for example, paclitaxel, also increases cardiotoxicity, despite enhanced treatment efficacy (14, 16). Since cardiotoxicity with active agents, including DOX and trastuzumab, has significantly limited the use of combination therapy against breast cancer, new therapeutic modalities to overcome this toxic effect are urgently needed.

In this study, CBR1 is shown to be a novel molecular target to enhance chemotherapeutic efficacy of DOX in breast cancer cells. It was clearly demonstrated that inhibition of CBR1 by chemical inhibitor, OH-PP-Me, increased anticancer effects of DOX in breast cancer cells. It was also observed that overexpression of CBR1 decreased DOX-induced anticancer effects in breast cancer cells, whereas CBR1 knockdown increased these effects. Our previous studies demonstrated that CBR1 had protective effects against oxidative stress in diverse conditions (17, 45). A recent report has also revealed that CBR1 induces doxorubicin resistance *via* reducing oxidative stress in diverse gastrointestinal cancer cells (26). Consistent with this concept, the present study found that suppression of CBR1 increased superoxide ($O_2^{\bullet-}$) levels after DOX treatment. Conversely, overexpression of CBR1 decreased superoxide ($O_2^{\bullet-}$) levels in breast cancer cells. These data indicate that CBR1 plays a regulatory role in apoptosis and cell survival *via* oxidative stress.

TABLE 2. EFFECTS OF DOX AND/OR OH-PP-ME ON CLINICAL BIOCHEMISTRY VALUES

Parameters	Reference range[a]	Control[a]	OH-pp-Me[a]	DOX[a]	OH-pp-Me + DOX[a]
GGT (U/L)	1.5–5	3.69 ± 0.26	2.77 ± 0.64	3.04 ± 0.28	2.21 ± 1.26
TP (g/dl)	3.5–7.2	5.13 ± 0.05	5.38 ± 0.21	4.46 ± 0.81	4.62 ± 0.39
ALB (g/dl)	2.5–3	2.96 ± 0.02	3.0 ± 0.06	2.47 ± 0.27	2.6 ± 0.16
ALP (U/L)	140–250	210.58 ± 32.49	238.21 ± 23.81	200.7 ± 27.64	169.20 ± 49.27
AST (U/L)	54–298	143.75 ± 14.62	189.05 ± 46.72	250.31 ± 103.29	179.39 ± 44.79
ALT (U/L)	17–77	40.79 ± 5.82	43.8 ± 5.99	45.03 ± 19.23	37.39 ± 4.52
T-BIL (mg/dl)	0–0.9	0.023 ± 0.012	0.05 ± 0.008	0.03 ± 0.035	0.054 ± 0.029
D-BIL (mg/dl)		0.01 ± 0.008	0.017 ± 0.007	0.018 ± 0.015	0.016 ± 0.008
T-CHOL (mg/dl)	90–135	102.77 ± 1.67	108.99 ± 6.25	75.80 ± 30.52	91.83 ± 10.06
HDL (mg/dl)		60.11 ± 1.04	63.55 ± 3.24	35.84 ± 17.00	42.71 ± 5.77
LDL (mg/dl)		4.02 ± 0.39	4.8 ± 0.40	11.33 ± 5.15	16.29 ± 5.27
LDH (U/L)		612.90 ± 23.93	659.23 ± 111.08	706.25 ± 96.54	755.23 ± 87.14

[a]Mean ± SE (range).
GGT, gamma-glutamyl transpeptidase; TP, total proteins; ALB, albumin; ALP, alkaline phosphatase; AST, aspartate aminotransferase; ALT, alanine aminotransferase; T-BIL, total bilirubin; D-BIL, direct bilirubin; T-CHOL, total cholesterol; HDL, high-density lipoproteins; LDL, low-density lipoproteins; LDH, lactate dehydrogenase.
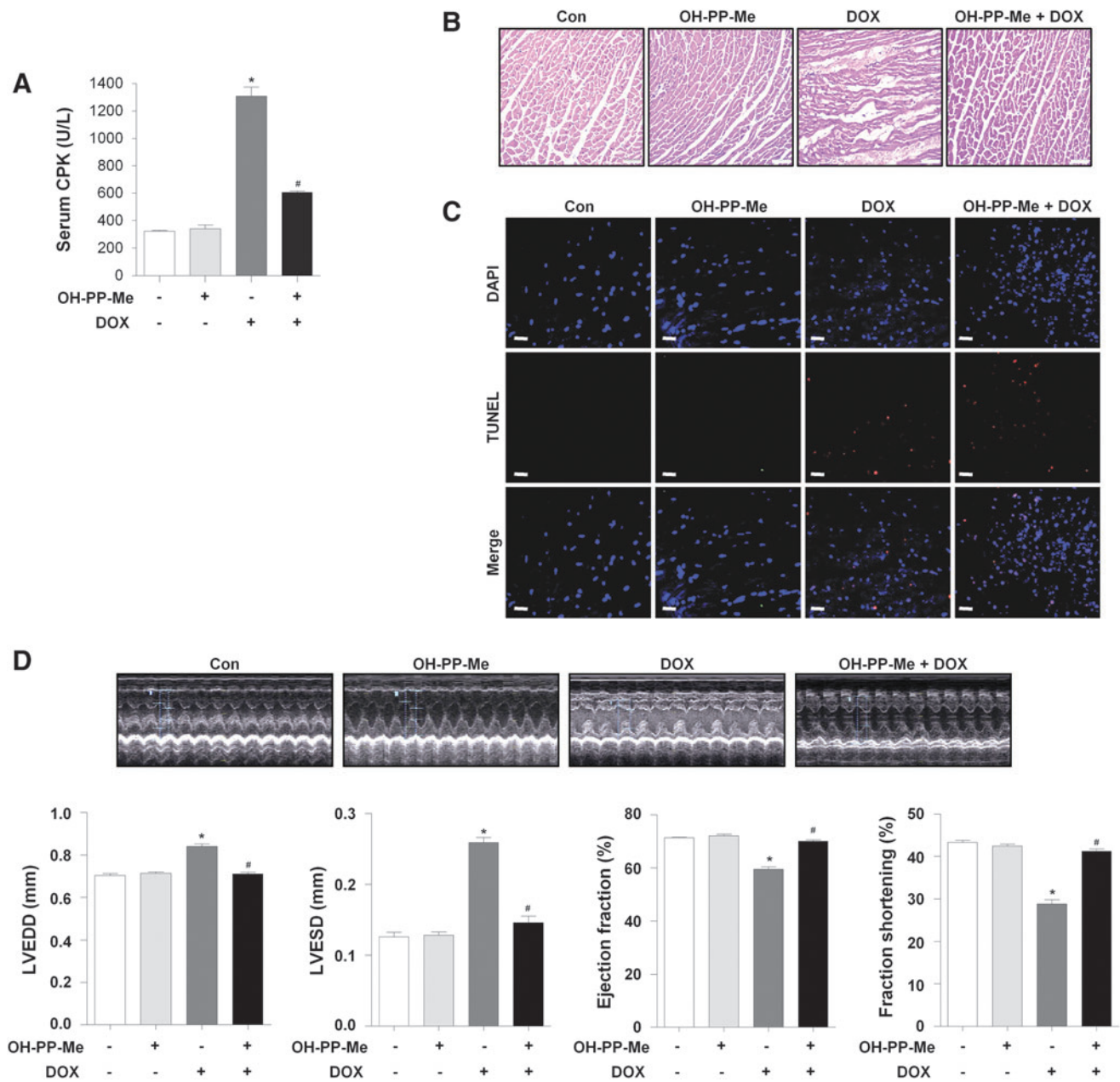
FIG. 7. Effect of OH-PP-Me on DOX-induced cardiotoxicity in rat. Rats were injected intraperitoneally with DOX (2.5 mg/kg) alone, OH-PP-Me (1.67 mg/kg) alone, or in combination every 2 days for 2 weeks. For the combination treatment, rats were injected with OH-PP-Me 1 h post-DOX injection. **(A)** CPK assay. *$p < 0.05$ *versus* untreated rats; [#]$p < 0.05$ *versus* DOX-injected rats. **(B)** H&E staining. Scale bar, 50 μm. **(C)** TUNEL staining. Nuclei were stained with DAPI. Scale bar, 20 μm. **(D)** Transthoracic echocardiography was used to measure cardiac function in rats. Representative M-mode echocardiograms were obtained from hearts with no treatment (Con), OH-PP-Me alone, DOX alone, and combination treatment (OH-PP-Me and DOX). Heart dimensions of left ventricular end-diastolic dimension (LVEDD), left ventricular end-systolic dimension (LVESD), the percentage of LV ejection fraction (%EF), and the percentage of LV fractional shortening (%FS) were determined. *$p < 0.05$ *versus* untreated rats; [#]$p < 0.05$ *versus* DOX-injected rats. To see this illustration in color, the reader is referred to the web version of this article at www.liebertpub.com/ars

Due to a lack of specificity, patients undergoing DOX treatment can develop several adverse effects, the most severe of which is cardiomyopathy, leading to heart failure (8). Therefore, DOX-induced cardiomyopathy limits its therapeutic application as an anticancer drug and, thus, continues to present a clinical dilemma in oncology and cardiology practices (41, 43). Recently, DOX was modified to evade these adverse effects. For example, pegylated liposomal DOX (PL-DOX) has shown a better pharmacokinetic profile and less cardiotoxicity than DOX itself (2, 28). However, PL-DOX causes severe skin toxicity due to the unique pharmacokinetics of circulating liposomes (33). Thus, there is still a strong need to improve the anticancer effects and to reduce other adverse effects of PL-DOX.

DOX-induced cardiotoxicity appears to be a multifactorial process, and numerous mechanisms have been proposed (6, 15, 31, 39). DOX generates the DOX-semiquinone that induces DNA damage and lipid peroxidation *via* ROS formation (30). On the contrary, it has been reported that carbonyl reduction of DOX to the secondary alcohol metabolite, DOXOL, contributes to severe cardiotoxicity (40). Since the metabolism of DOX involves CBR1, the present study hypothesized that a CBR1 inhibitor, for example, OH-PP-Me, might prevent DOX-induced cardiotoxicity. In fact, our results showed this to be the case, that is, inhibition of CBR1 augments chemotherapy efficacy and attenuates cardiotoxicity by blocking DOX reduction to DOXOL.

In summary, the current study demonstrated that inhibition of CBR1 enhances chemotherapeutic efficacy of DOX and attenuates cardiotoxicity by blocking DOX reduction to DOXOL. Therefore, we propose that development of the CBR1 inhibitors that can be administered into cancer patients will pave the new way for better application of DOX in oncology clinics.

Materials and Methods

Materials

Dulbecco's modified Eagle's medium (DMEM), Roswell Park Memorial Institute medium 1640 (RPMI1640), penicillin/streptomycin, and fetal bovine serum (FBS) were purchased from Corning Cellgro (Manassas, VA). The antibody against CBR1 was purchased from Abcam (Cambridge, MA). Antibodies against cleaved caspase-3, caspase-7, and Bax were acquired from Cell Signaling Technology, Inc. (Danvers, MA). PARP and actin were purchased from Santa Cruz Biotechnology (Santa Cruz, CA). Doxorubicin, hydrogen peroxide (H_2O_2), dihydroethidium (DHE), propidium iodide, RNase-A, and Mayer's hematoxylin were acquired from Sigma-Aldrich (St. Louis, MO). Doxorubicin for animal experiments was purchased from Dong-A Pharmaceutical Co. (Seoul, Korea). 2′-7′-5-(and-6)-Chloromethyl-2′,7′-dichlorodihydrofluorescein diacetate (CM-H2DCFDA) and trypan blue were acquired from Life Technologies Co. (Carlsbad, CA). The Cell Counting Kit-8 (CCK-8) was purchased from Enzo Life Sciences, Inc. (Farmingdale, NY).

Cell culture

Human breast cancer cells (MDA-MB 157, MDA-MB-436, MCF-7, and MCF10A) were obtained from the American Type Culture Collection (ATCC; Rockville, MD). MDA-MB 157 cells were maintained in DMEM supplemented with 10% heat-inactivated FBS and $100\,\mu g/ml$ penicillin/streptomycin. MDA-MB436 and MCF-7 cells were maintained in RPMI1640 supplemented with 10% heat-inactivated FBS and $100\,\mu g/ml$ penicillin/streptomycin. MCF10A cells were maintained in DMEM/F12 with 5% horse serum, $2\,mM$ L-glutamine, EGF $20\,ng/ml$, insulin $10\,\mu g/ml$, hydrocortisone $0.5\,\mu g/ml$, cholera toxin 0.1, and $100\,\mu g/ml$ penicillin/streptomycin.

Assessment of cell proliferation

To assess the effects of combined treatment on cell proliferation, CCK-8 assays were carried out in 24-well plates, following the manufacturer's instructions. The absorbance was measured at 450 nm using a microplate reader (Bio-Rad Laboratories, Inc., Tokyo, Japan).

Cell viability

Cell viability was detected using Vi-CELL XR (Beckman Coulter, Inc., Brea, CA) after trypan blue staining. Cell survival was expressed as the relative percentage of viable cell numbers.

Cell cycle analysis

Cells were grown to 80% confluence, harvested, rinsed with PBS, and then fixed in 75% ethanol for 1 h at 4°C. The fixed cells were centrifuged and suspended in 0.5 ml PBS containing 0.05 mg/ml propidium iodide and 0.2 mg/ml RNase-A, and then incubated at 37°C for 15 min. Red fluorescence (580–630 nm) of propidium iodide was measured in the FL-2 channel, and 30,000 events were collected for each sample. The data were analyzed with CellQuest software (Beckman Coulter, Inc.).

Clonogenic colony formation assay

Cells were plated at a concentration of 500 cells/well in a 6-well plate and allowed to form colonies for 14 days. The colonies were fixed and stained with crystal violet dye (0.5% in methanol) at room temperature after they were washed in PBS. Cells were washed with water, and plates were photographed with an image scanner. Crystal violet was resolved from colonies by methanol and measured at 540 nm. Based on the absorbance at 540 nm, survival rates were expressed as a percentage relative to DMSO-treated control from three independent experiments.

TUNEL assay for apoptosis

Cells. Breast cancer cells were fixed for 30 min in 4% paraformaldehyde. The fragmented DNA in the cells undergoing apoptosis was detected using the DeadEnd™ Colorimetric TUNEL System (Promega Corp., Madison, WI). The TUNEL-positive nuclei (dark brown) in breast cancer cells were observed using a normal white light microscope (Olympus, Tokyo, Japan).

Tissues. The tumor and heart tissue sections from animal models were used for the TUNEL assay and the FragEL™ DNA Fragmentation Detection Kit (Merck KGaA, Darmstadt, Germany). Staining for the TUNEL assay was performed following the manufacturer's protocol. Incorporated fluorophores were examined with a confocal microscope (Carl Zeiss Microscopy GmbH, Göttingen, Germany) using appropriate excitation wavelengths and filter sets.

Quantification was performed by counting the number of TUNEL-positive cells in at least five random fields. The TUNEL-positive cells are expressed as a percentage of the total number of cells per field.

ROS analysis

Intracellular superoxide ($O2^{\bullet-}$) levels were measured with DHE using a flow cytometer (Beckman Coulter, Inc.). Cells were incubated with $25\,\mu M$ DHE at 37°C for 20 min. The mean DHE fluorescence intensity was measured with excitation 488 nm and emission 525 nm.

The H_2O_2 levels were measured using CM-H2DCFDA. Cells were incubated with $5\,\mu M$ CM-H2DCFDA at 37°C for 30 min. The mean CM-H2DCFDA fluorescence intensity was measured with excitation 488 nm and emission 525 nm.

Establishment of stable cell lines

MDA-MB-157 and MCF7 cells were transfected with pcDNA3 (Mock) or pcDNA3-CBR1 wild-type (CBR1/WT) plasmid using TransIT-BrCa transfection reagent (Mirus Corp., Madison, WI), according to the manufacturer's instructions. Cells transfected with pcDNA3 plasmid alone without the CBR1 gene (Mock) were used as the control.

Two independent small hairpin RNAs (shRNAs) specific to CBR1 (pLKO-shCBR1) were purchased from Sigma Aldrich; #1 shCBR1, CCGGCAAGCTGAAGTGACGATGAAACT CGAGTTTCATCGTCACTTCAGCTTGTTTTTG; #2 shCBR1, CCGGCCATGGACAATT TGTTTCAGACTCGAGTCTG AAACAA ATTGTCCATGGTTTTTG. Cells transfected with the pLKO plasmid without the CBR1 shRNA (scrambled [SC]) were used as the control. For stable transfection, cells were cultured in selective medium with 600 μg/ml G418 or 20 μg/ml puromycin for 2 weeks. Then, drug-resistant individual clones were isolated and incubated for further amplification in the presence of selective medium. The CBR1 expression levels in these stable cells were confirmed by immunoblotting. To re-express a functional CBR1, two pEGFP-N1-CBR1/wt plasmids were constructed containing a ''wobble'' mutant cDNA encoding human CBR1 with synonymous point mutations within the two shRNA target sequences (5′- CCA TTC CAC ATC CAG GCA GAG −3′ for shCBR1 #1, GFP-CBR1/wt #1; 5′- ACT GAG CTC TTG CCA TTT ATC −3′ for shCBR1 #2, GFP-CBR1/wt 2 with mutation sites underlined) and transfected into MDA-MB-157 and MCF7 cell clones harboring the CBR1 shRNA.

Implantation tumor nude mice

Female athymic nude mice (Foxn1 nu/nu) aged 4 weeks were purchased from Harlan (Udine, Italy) and were allowed to acclimate for 1 week. The animal protocol was approved by the Institutional Animal Care and Use Committee of Kyung Hee University (Seoul, Korea). To establish implantation tumor nude mice of breast cancer, 10^7 MDA-MB-157 human breast cancer cells in 0.2 ml PBS were injected into the mammary fat pad. Two groups of the experimental mice were established; one were mice that developed tumors and the other were normal healthy mice. The two groups were further divided into different treatment groups as follows: Group 1: Untreated control; Group 2: OH-PP-Me 1.67 mg/kg, 6 times (i.p.); Group 3: DOX 2.5 mg/kg, 6 times (i.p.); Group 4: OH-PP-Me 1.67 mg/kg, and after 1 h, DOX 2.5 mg/kg, 6 times (i.p.).

After 2 weeks of treatment, tumor and heart tissues were collected for histological and immunohistochemical analysis, while blood samples were collected for the CPK activity assay.

Determination of cardiac function in rat

The rats were divided into three treatment groups (DOX alone (2.5 mg/kg × 6 times, i.p.), 3-(7-isopropyl-4-(methylamino)-7H-pyrrolo[2,3-d]pyrimidin-5yl)phenol (OH-PP-Me) alone (1.67 mg/kg × 6 times, i.p.), and a combination of OH-PP-Me and DOX), and one group as an untreated control. For the combination treatment group, rats were injected with OH-PP-Me 1 h after the injection of DOX. After 4 weeks, the rats underwent echocardiography, and then blood and heart tissue samples were collected for further analysis. Animal experiments were conducted according to the protocol approved by the Institutional Animal Care and Use Committee of Kyung Hee University (Seoul, Korea). Male Sprague Dawley rats (8–9 weeks old) were purchased from Orient Bio, Inc. (Sungnam, Korea).

Measurement of CPK activity

CPK activities were measured after treatment by using a CPK test kit (Abnova Corp., Taipei, Taiwan). One unit of CPK was defined as the reduction of 1 μM NAD$^+$ to NADH per minute.

Histological analysis of animal models

The tumors and hearts were isolated from the animals of each group. Paraffin-embedded, 5-μm-thick heart tissue sections were used. Routine H&E-stained sections were examined to ensure the structural integrity of the tissues using a normal white light microscope.

Echocardiography

Following anesthetization, rats were shaved and placed in the supine position. Transthoracic echocardiography was performed to obtain two-dimensional M-mode images, using a 13-MHz linear probe (Vivid FiVe; GE Medical Systems, Milwaukee, WI). From M-the mode images, LVEDD and LVESD were determined according to the standard method of the American Society of Echocardiography. All measurements were averaged from values of three cardiac cycles. LV FS was calculated as (LVEDD—LVESD)/LVEDD × 100. EF was calculated using the Teichholz formula.

Western blot analyses

Western blot analyses were performed using whole-cell extracts as previously described (48). Protein concentrations of lysates were measured using a Bio-Rad DC protein assay (Bio-Rad Laboratories, Inc.). For immunoblotting, the proteins were separated on 8–15% SDS-PAGE and transferred onto nitrocellulose membranes (Pall Corporation, Washington, NY). After blocking, primary antibodies were diluted according to the manufacturer's instructions. The blotted proteins were detected with an enhanced chemiluminescence detection system (Santa Cruz Biotechnology, Dallas, TX). Actin was used as a loading control.

Statistical analysis

The results are expressed as the mean ± standard error of the mean of at least three independent experiments. The differences between two means were analyzed for significance by the Student's t-test (SPSS for Windows; version 22.0, SPSS, Inc., Chicago, IL). $p < 0.05$ were considered significant.

Acknowledgments

Author Disclosure Statement

No competing financial interests exist.

References

1. Abbott A. Laboratory animals: the Renaissance rat. *Nature* 428: 464–466, 2004.
2. Alberts DS, Muggia FM, Carmichael J, Winer EP, Jahanzeb M, Venook AP, Skubitz KM, Rivera E, Sparano JA, DiBella NJ, Stewart SJ, Kavanagh JJ, and Gabizon AA. Efficacy and safety of liposomal anthracyclines in phase I/II clinical trials. *Semin Oncol* 31: 53–90, 2004.
3. Arcamone F, Cassinelli G, Fantini G, Grein A, Orezzi P, Pol C, and Spalla C. Adriamycin, 14-hydroxydaunomycin, a new antitumor antibiotic from S. peucetius var. caesius. Reprinted from biotechnology and bioengineering, XI: 1101–1110, 1969. *Biotechnol Bioeng* 67: 704–713, 2000.
4. Atalla A and Maser E. Carbonyl reduction of the tobacco-specific nitrosamine 4-(methylnitrosamino)-1-(3-pyridyl)-1-butanone (NNK) in cytosol of mouse liver and lung. *Toxicology* 139: 155–166, 1999.
5. Banerjee I, Fuseler JW, Price RL, Borg TK, and Baudino TA. Determination of cell types and numbers during cardiac development in the neonatal and adult rat and mouse. *Am J Physiol Heart Circ Physiol* 293: H1883–H1891, 2007.
6. Blanco JG, Sun CL, Landier W, Chen L, Esparza-Duran D, Leisenring W, Mays A, Friedman DL, Ginsberg JP, Hudson MM, Neglia JP, Oeffinger KC, Ritchey AK, Villaluna D, Relling MV, and Bhatia S. Anthracycline-related cardiomyopathy after childhood cancer: role of polymorphisms in carbonyl reductase genes—a report from the Children's Oncology Group. *J Clin Oncol* 30: 1415–1421, 2012.
7. Boucek RJ, Jr., Olson RD, Brenner DE, Ogunbunmi EM, Inui M, and Fleischer S. The major metabolite of doxorubicin is a potent inhibitor of membrane-associated ion pumps. A correlative study of cardiac muscle with isolated membrane fractions. *J Biol Chem* 262: 15851–15856, 1987.
8. Buja LM, Ferrans VJ, Mayer RJ, Roberts WC, and Henderson ES. Cardiac ultrastructural changes induced by daunorubicin therapy. *Cancer* 32: 771–788, 1973.
9. Carrick S, Parker S, Thornton CE, Ghersi D, Simes J, and Wilcken N. Single agent *versus* combination chemotherapy for metastatic breast cancer. *Cochrane Database Syst Rev* CD003372, 2009.
10. Carvalho FS, Burgeiro A, Garcia R, Moreno AJ, Carvalho RA, and Oliveira PJ. Doxorubicin-induced cardiotoxicity: from bioenergetic failure and cell death to cardiomyopathy. *Med Res Rev* 34: 106–135, 2014.
11. Forrest GL, Gonzalez B, Tseng W, Li X, and Mann J. Human carbonyl reductase overexpression in the heart advances the development of doxorubicin-induced cardiotoxicity in transgenic mice. *Cancer Res* 60: 5158–5164, 2000.
12. Gatenby RA. A change of strategy in the war on cancer. *Nature* 459: 508–509, 2009.
13. Gavelova M, Hladikova J, Vildova L, Novotna R, Vondracek J, Krcmar P, Machala M, and Skalova L. Reduction of doxorubicin and oracin and induction of carbonyl reductase in human breast carcinoma MCF-7 cells. *Chem Biol Interact* 176: 9–18, 2008.
14. Gehl J, Boesgaard M, Paaske T, Vittrup Jensen B, and Dombernowsky P. Combined doxorubicin and paclitaxel in advanced breast cancer: effective and cardiotoxic. *Ann Oncol* 7: 687–693, 1996.
15. Gewirtz DA. A critical evaluation of the mechanisms of action proposed for the antitumor effects of the anthracycline antibiotics adriamycin and daunorubicin. *Biochem Pharmacol* 57: 727–741, 1999.
16. Gianni L, Munzone E, Capri G, Fulfaro F, Tarenzi E, Villani F, Spreafico C, Laffranchi A, Caraceni A, Martini C, et al. Paclitaxel by 3-hour infusion in combination with bolus doxorubicin in women with untreated metastatic breast cancer: high antitumor efficacy and cardiac effects in a dose-finding and sequence-finding study. *J Clin Oncol* 13: 2688–2699, 1995.
17. Jang M, Kim Y, Won H, Lim S, K R J, Dashdorj A, Min YH, Kim SY, Shokat KM, Ha J, and Kim SS. Carbonyl reductase 1 offers a novel therapeutic target to enhance leukemia treatment by arsenic trioxide. *Cancer Res* 72: 4214–4224, 2012.
18. Johnson PJ, Dobbs N, Kalayci C, Aldous MC, Harper P, Metivier EM, and Williams R. Clinical efficacy and toxicity of standard dose adriamycin in hyperbilirubinaemic patients with hepatocellular carcinoma: relation to liver tests and pharmacokinetic parameters. *Br J Cancer* 65: 751–755, 1992.
19. Kaklamani VG and Gradishar WJ. Epirubicin *versus* doxorubicin: which is the anthracycline of choice for the treatment of breast cancer? *Clin Breast Cancer* 4 Suppl 1: S26–S33, 2003.
20. King PD and Perry MC. Hepatotoxicity of chemotherapy. *Oncologist* 6: 162–176, 2001.
21. Klement G, Baruchel S, Rak J, Man S, Clark K, Hicklin DJ, Bohlen P, and Kerbel RS. Continuous low-dose therapy with vinblastine and VEGF receptor-2 antibody induces sustained tumor regression without overt toxicity. *J Clin Invest* 105: R15–R24, 2000.
22. Lee V, Randhawa AK, and Singal PK. Adriamycin-induced myocardial dysfunction in vitro is mediated by free radicals. *Am J Physiol* 261: H989–H995, 1991.
23. Lefrak EA, Pitha J, Rosenheim S, and Gottlieb JA. A clinicopathologic analysis of adriamycin cardiotoxicity. *Cancer* 32: 302–314, 1973.
24. Lopez de Cerain A, Marin A, Idoate MA, Tunon MT, and Bello J. Carbonyl reductase and NADPH cytochrome P450 reductase activities in human tumoral *versus* normal tissues. *Eur J Cancer* 35: 320–324, 1999.
25. Lotrionte M, Palazzoni G, Natali R, Comerci G, Abbate A, Loperfido F, and Biondi-Zoccai G. Assessment of left ventricular systolic dysfunction by tissue Doppler imaging to detect subclinical cardiomyopathy early after anthracycline therapy. *Minerva Cardioangiol* 55: 711–720, 2007.
26. Matsunaga T, Kezuka C, Morikawa Y, Suzuki A, Endo S, Iguchi K, Miura T, Nishinaka T, Terada T, El-Kabbani O, Hara A, and Ikari A. Up-regulation of carbonyl reductase 1 renders development of doxorubicin resistance in human gastrointestinal cancers. *Biol Pharm Bull* 38: 1309–1319, 2015.
27. Mauri D, Polyzos NP, Salanti G, Pavlidis N, and Ioannidis JP. Multiple-treatments meta-analysis of chemotherapy and targeted therapies in advanced breast cancer. *J Natl Cancer Inst* 100: 1780–1791, 2008.
28. Menna P, Paz OG, Chello M, Covino E, Salvatorelli E, and Minotti G. Anthracycline cardiotoxicity. *Expert Opin Drug Saf* 11: S21–S36, 2012.
29. Minotti G, Menna P, Salvatorelli E, Cairo G, and Gianni L. Anthracyclines: molecular advances and pharmacologic developments in antitumor activity and cardiotoxicity. *Pharmacol Rev* 56: 185–229, 2004.
30. Minotti G, Ronchi R, Salvatorelli E, Menna P, and Cairo G. Doxorubicin irreversibly inactivates iron regulatory proteins 1 and 2 in cardiomyocytes: evidence for distinct metabolic pathways and implications for iron-mediated cardiotoxicity of antitumor therapy. *Cancer Res* 61: 8422–8428, 2001.
31. Minotti G, Salvatorelli E, and Menna P. Pharmacological foundations of cardio-oncology. *J Pharmacol Exp Ther* 334: 2–8, 2010.

32. Novotna R, Wsol V, Xiong G, and Maser E. Inactivation of the anticancer drugs doxorubicin and oracin by aldo-keto reductase (AKR) 1C3. *Toxicol Lett* 181: 1–6, 2008.

33. O'Brien ME, Wigler N, Inbar M, Rosso R, Grischke E, Santoro A, Catane R, Kieback DG, Tomczak P, Ackland SP, Orlandi F, Mellars L, Alland L, and Tendler C. Reduced cardiotoxicity and comparable efficacy in a phase III trial of pegylated liposomal doxorubicin HCl (CAELYX/Doxil) *versus* conventional doxorubicin for first-line treatment of metastatic breast cancer. *Ann Oncol* 15: 440–449, 2004.

34. Olson LE, Bedja D, Alvey SJ, Cardounel AJ, Gabrielson KL, and Reeves RH. Protection from doxorubicin-induced cardiac toxicity in mice with a null allele of carbonyl reductase 1. *Cancer Res* 63: 6602–6606, 2003.

35. Olson RD, Mushlin PS, Brenner DE, Fleischer S, Cusack BJ, Chang BK, and Boucek RJ, Jr. Doxorubicin cardiotoxicity may be caused by its metabolite, doxorubicinol. *Proc Natl Acad Sci U S A* 85: 3585–3589, 1988.

36. Oppermann U. Carbonyl reductases: the complex relationships of mammalian carbonyl- and quinone-reducing enzymes and their role in physiology. *Annu Rev Pharmacol Toxicol* 47: 293–322, 2007.

37. Polyak K. Heterogeneity in breast cancer. *J Clin Invest* 121: 3786–3788, 2011.

38. Salvatorelli E, De Tursi M, Menna P, Carella C, Massari R, Colasante A, Iacobelli S, and Minotti G. Pharmacokinetics of pegylated liposomal doxorubicin administered by intraoperative hyperthermic intraperitoneal chemotherapy to patients with advanced ovarian cancer and peritoneal carcinomatosis. *Drug Metab Dispos* 40: 2365–2373, 2012.

39. Salvatorelli E, Guarnieri S, Menna P, Liberi G, Calafiore AM, Mariggio MA, Mordente A, Gianni L, and Minotti G. Defective one- or two-electron reduction of the anticancer anthracycline epirubicin in human heart. Relative importance of vesicular sequestration and impaired efficiency of electron addition. *J Biol Chem* 281: 10990–11001, 2006.

40. Salvatorelli E, Menna P, Gonzalez Paz O, Surapaneni S, Aukerman SL, Chello M, Covino E, Sung V, and Minotti G. Pharmacokinetic characterization of amrubicin cardiac safety in an ex vivo human myocardial strip model. II. Amrubicin shows metabolic advantages over doxorubicin and epirubicin. *J Pharmacol Exp Ther* 341: 474–483, 2012.

41. Shan K, Lincoff AM, and Young JB. Anthracycline-induced cardiotoxicity. *Ann Intern Med* 125: 47–58, 1996.

42. Siegel RL, Miller KD, and Jemal A. Cancer statistics, 2015. *CA Cancer J Clin* 65: 5–29, 2015.

43. Singal PK and Iliskovic N. Doxorubicin-induced cardiomyopathy. *N Engl J Med* 339: 900–905, 1998.

44. Slamon DJ, Leyland-Jones B, Shak S, Fuchs H, Paton V, Bajamonde A, Fleming T, Eiermann W, Wolter J, Pegram M, Baselga J, and Norton L. Use of chemotherapy plus a monoclonal antibody against HER2 for metastatic breast cancer that overexpresses HER2. *N Engl J Med* 344: 783–792, 2001.

45. Tak E, Lee S, Lee J, Rashid MA, Kim YW, Park JH, Park WS, Shokat KM, Ha J, and Kim SS. Human carbonyl reductase 1 upregulated by hypoxia renders resistance to apoptosis in hepatocellular carcinoma cells. *J Hepatol* 54: 328–339, 2011.

46. Von Hoff DD, Layard MW, Basa P, Davis HL, Jr., Von Hoff AL, Rozencweig M, and Muggia FM. Risk factors for doxorubicin-induced congestive heart failure. *Ann Intern Med* 91: 710–717, 1979.

47. Weiss RB. The anthracyclines: will we ever find a better doxorubicin? *Semin Oncol* 19: 670–686, 1992.

48. Won H, Lim S, Jang M, Kim Y, Rashid MA, Jyothi KR, Dashdorj A, Kang I, Ha J, and Kim SS. Peroxiredoxin-2 upregulated by NF-kappaB attenuates oxidative stress during the differentiation of muscle-derived C2C12 cells. *Antioxid Redox Signal* 16: 245–261, 2012.

49. Yang XH, Sladek TL, Liu X, Butler BR, Froelich CJ, and Thor AD. Reconstitution of caspase 3 sensitizes MCF-7 breast cancer cells to doxorubicin- and etoposide-induced apoptosis. *Cancer Res* 61: 348–354, 2001.

50. Yen HC, Oberley TD, Vichitbandha S, Ho YS, and St Clair DK. The protective role of manganese superoxide dismutase against adriamycin-induced acute cardiac toxicity in transgenic mice. *J Clin Invest* 98: 1253–1260, 1996.

51. Zhang S, Liu X, Bawa-Khalfe T, Lu LS, Lyu YL, Liu LF, and Yeh ET. Identification of the molecular basis of doxorubicin-induced cardiotoxicity. *Nat Med* 18: 1639–1642, 2012.

52. Zhou S, Starkov A, Froberg MK, Leino RL, and Wallace KB. Cumulative and irreversible cardiac mitochondrial dysfunction induced by doxorubicin. *Cancer Res* 61: 771–777, 2001.

Address correspondence to:
Dr. Sung Soo Kim
Department of Biochemistry and Molecular Biology
School of Medicine
Kyung Hee University
26 Kyungheedae-ro, Dongdaemun-gu
Seoul 02447
Republic of Korea

E-mail: sgskim@khu.ac.kr

Abbreviations Used

AKR1A1	= aldo-keto reductase 1A1
AKR1C3	= aldo-keto reductase 1C3
CBR1	= carbonyl reductase 1
CCK-8	= cell counting kit-8
CM-H2DCFDA	= 2′-7′-5-(and-6)-chloromethyl-2′,7′-dichlorodihydrofluorescein diacetate
CPK	= serum creatine phosphokinase
DHE	= dihydroethidium
DMEM	= Dulbecco's modified Eagle's medium
DOX	= doxorubicin
DOXOL	= doxorubicinol
EF	= ejection fraction
FBS	= fetal bovine serum
FS	= fractional shortening
H&E	= hematoxylin and eosin
LVEDD	= left ventricular end-diastolic dimension
LVESD	= left ventricular end-systolic dimension
NAC	= N-acetyl-l-cysteine
OH-PP-Me	= 3-(7-isopropyl-4-(methylamino)-7H-pyrrolo[2,3-d]pyrimidin-5yl)phenol
PL-DOX	= pegylated liposomal doxorubicin
ROS	= reactive oxygen species
shRNA	= small hairpin RNA
Topo II	= topoisomerase II
TUNEL	= terminal transferase dUTP nick end-labeling